Bifurcations of Periodic Trajectories in Non-integrable Hamiltonian Systems with Two Degrees of Freedom: Numerical and Analytical Results

M. A. M. DE AGUIAR* AND C. P. MALTA

*Instituto de Física, Universidade de São Paulo,
C.P. 20516, 01498, São Paulo, SP, Brazil*

M. BARANGER

*Center for Theoretical Physics, Laboratory for Nuclear Science and Department of Physics,
Massachusetts Institute of Technology, Cambridge, Massachusetts 02139*

AND

K. T. R. DAVIES

*Physics Division, Oak Ridge National Laboratory,
Oak Ridge, Tennessee 37831*

Numerical and analytical studies of the types of period n-upling bifurcations undergone by classsical periodic trajectories of non-integrable Hamiltonians with two degrees of freedom are made. The Hamiltonians studied possess time reversal and reflexion symmetries and we found that these symmetries give rise to additional types of period n-upling bifurcations. The analytical study explains most of the numerically observed bifurcations.   © 1987 Academic Press, Inc.

1. INTRODUCTION

In a recently published paper [1], two of us presented the results of an extensive numerical investigation of the periodic solutions of a two-dimensional non-integrable Hamiltonian system with two degrees of freedom. In this paper, we show similar results for another potential. More importantly, we also present a complete study of the bifurcations, or branchings, undergone by the periodic trajectories. We show that the empirically observed bifurcations correspond exactly to the results of

---

* Present address: Center for Theoretical Physics, MIT, Cambridge, MA 02139.

167

an analytic study of possible types of bifurcations for a Hamiltonian possessing some symmetries.

The Hamiltonian considered here is

$$H = \tfrac{1}{2}p_x^2 + \tfrac{1}{2}p_y^2 + \tfrac{1}{2}x^2 + \tfrac{3}{2}y^2 - x^2 y + \tfrac{1}{12}x^4 \tag{1.1}$$

and our code name for it is MARTA. It has the same analytical form as the NELSON Hamiltonian of Ref. [1], but with different coefficients. Contours of the MARTA potential are shown in Fig. 1. It differs from the Nelson potential in having two saddle points, and in the fact that it goes to $-\infty$ is some directions. Like NELSON, MARTA has $x \to -x$ symmetry. Taken together with time-reversal, this means that there are two distinct symmetries which can be possessed by the families of periodic trajectories. We originally chose MARTA because it resembled the Hénon Heiles [2] potential, but with less symmetry. The high symmetry of Hénon–Heiles was thought, at the time, to bring complications in the search for low-energy periodic families.

We shall present the numerical results in very much the same way as in Ref. [1]. In particular, we shall draw E–τ plots of the periodic families. As in Ref. [1], we shall emphasize the properties of the monodromy matrix, or M-matrix (also called Liapunov matrix) [3]. This is the symplectic matrix which connects an infinitesimal change in initial conditions to the corresponding change at the end of one period.
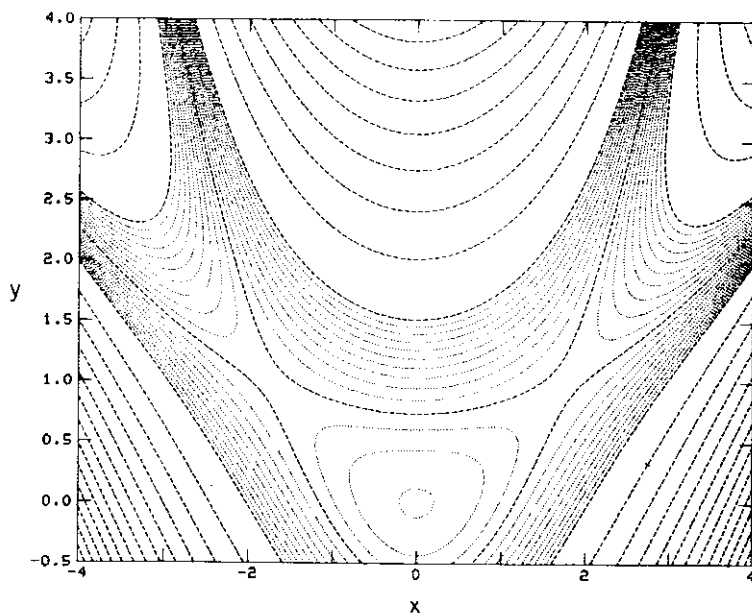

FIG. 1. Equipotential lines of the MARTA potential.

The textbooks, such as Ref. [3], derive the properties of the M-matrix in the context of systems evolving in continuous time. We show in Section 2 how these well-known properties are modified by the discretization of the time axis which is necessary to perform the numerical calculations.

The numerical results themselves were obtained by the same method [4] as those of Ref. [1]. We have calculated roughly 2000 periodic trajectories comprising roughly 50 families for MARTA. Some of these results are shown in Section 3. Two additional two-dimensional potentials have been investigated thoroughly by this method, with results to be published later. They are

$$\text{MARCO [5]:} \quad V(x, y) = \tfrac{1}{4}(x^2 + y^2 - 1)^2 + \tfrac{1}{2}\mu y(3 - x^2 - y^2), \qquad \mu = 0.15$$

$$\text{DELFI [6]:} \quad V(x, y) = \tfrac{1}{4}(x^2 + y^2)^2 + \tfrac{1}{4}\mu x^3(y - 1) - y(x^2 + y^2)$$
$$+ \tfrac{1}{2}(x^2 + 3y^2), \qquad \mu = (\tfrac{128}{27})^{1/2}.$$

Section 4 contains a complete summary of the possible types of branchings in the families of periodic trajectories, for Hamiltonians possessing 0, 1, or 2 symmetries, as revealed by our numerical studies and those of Refs. [1, 5, 6]. An analytical study of this subject was carried out long ago by Meyer [7], but he confined himself to the generic case of Hamiltonians without symmetry. In Section 5 we extend the work of Meyer to include Hamiltonians with time-reversal symmetry and space-reflexion symmetry, and we find that these two symmetries are responsible for several interesting additional types of branchings, all of which show up in the numerical work.

We close this section by recalling one important motivation for this type of work, which is the quantization of many-body systems. Many of the more tractable approximations to many-body dynamics have a classical aspect to them; they consist of many-body wave packets following classical-like trajectories. The time-dependent Hartree–Fock and other time-dependent mean field approximations are of this type [8]. It is now well-known that such approximations can be generated in a general way by picking a wave-packet-like wavefunction depending on appropriate time-dependent parameters; when such a trial function is introduced in the time-dependent variational principle, the parameters are found to satisfy classical Hamiltonian equations [9].

2. The Discretized Monodromy Matrix

We shall study the discretized monodromy matrix for a two-dimensional Hamiltonian of the form

$$H(x, p_x, y, p_y) = \frac{p_x^2}{2} + \frac{p_y^2}{2} + V(x, y). \tag{2.1}$$

Extension to higher dimensionality is immediate. Extension to other types of Hamiltonians is possible. Newton's equations of motion for (2.1) are

$$\ddot{x} = -\frac{\partial V(x, y)}{\partial x} = -V_x(x, y),$$

$$\ddot{y} = -\frac{\partial V(x, y)}{\partial y} = -V_y(x, y), \tag{2.2}$$

a dot meaning a derivative with respect to time.

The M-matrix [3] gives the change in the solution of (2.2) after one period, in terms of the change in the initial conditions. It is therefore quite suitable for an iterative numerical procedure that produces a periodic solution of (2.2) starting from a periodic approximation to it. Such a procedure is decreibed in Ref. [4]. Here we shall confine ourselves to studying the monodromy matrix of a periodic trajectory which is already an exact solution.

Since we are doing numerical work, however, we must discretize Eq. (2.2). Let us specify the trajectory by N points equally spaced in time (x_n, y_n), $n = 0, 1, 2, ..., N-1$. Let ε be the time step and $\tau = N\varepsilon$ the period. Periodicity is expressed by

$$(x_0, y_0) = (x_N, y_N), \qquad (x_1, y_1) = (x_{N+1}, y_{N+1}). \tag{2.3}$$

We use the simplest discretization of (2.2), namely

$$x_{n+1} - 2x_n + x_{n-1} + \varepsilon^2 V_x(x_n, y_n) = 0,$$

$$y_{n+1} - 2y_n + y_{n-1} + \varepsilon^2 V_y(x_n, y_n) = 0. \tag{2.4}$$

The application of our numerical method yields an exact periodic solution (x_n, y_n) of Eqs. (2.4) for a given ε, and in the following we shall assume that this has been done.

Suppose now that we want to look for another solution $(x_n + \delta x_n, y_n + \delta y_n)$ of (2.4) in the vicinity of the first. This solution will generally be non-periodic. To obtain it, we linearize (2.4) in the vicinity of the original solution, assuming δx_n and δy_n small:

$$\delta x_{n+1} - 2\delta x_n + \delta x_{n-1} + \varepsilon^2 V_{xx}(x_n, y_n)\, \delta x_n + \varepsilon^2 V_{xy}(x_n, y_n)\, \delta y_n = 0$$

$$\delta y_{n+1} - 2\delta y_n + \delta y_{n-1} + \varepsilon^2 V_{xy}(x_n, y_n)\, \delta x_n + \varepsilon^2 V_{yy}(x_n, y_n)\, \delta y_n = 0. \tag{2.5}$$

Defining the vector

$$Z_n = \begin{pmatrix} \delta x_n \\ \delta y_n \\ \delta x_{n-1} \\ \delta y_{n-1} \end{pmatrix}. \tag{2.6}$$

we can express Eqs. (2.5) in the form

$$Z_{n+1} = U_n Z_n,$$ (2.7)

where U_n is a 4×4 matrix which, written in terms of 2×2 blocks, looks like

$$U_n = \begin{pmatrix} P_n & -1 \\ 1 & 0 \end{pmatrix},$$ (2.8)

with

$$P_n \equiv \begin{pmatrix} 2 - \varepsilon^2 V_{xx}(x_n, y_n) & -\varepsilon^2 V_{xy}(x_n, y_n) \\ -\varepsilon^2 V_{yx}(x_n, y_n) & 2 - \varepsilon^2 V_{yy}(x_n, y_n) \end{pmatrix}.$$ (2.9)

Using (2.7) recurrently we get

$$Z_{N+1} = M_1 Z_1,$$ (2.10)

where M_1 is the discretized monodromy matrix, given by

$$M_1 = U_N U_{N-1} \cdots U_2 U_1.$$ (2.11)

The inverse of U_n is easily seen to be

$$U_n^{-1} = \begin{pmatrix} 0 & 1 \\ -1 & P_n \end{pmatrix}$$ (2.12)

and it can be immediately verified that U_n has *the symplectic property*

$$U_n^{-1} = \Lambda U_n^{\mathrm{T}} \Lambda^{-1},$$ (2.13)

where Λ is the 4×4 matrix

$$\Lambda = \begin{pmatrix} 0 & 1 \\ -1 & 0 \end{pmatrix}$$ (2.14)

and the superscript T denotes transposition. The matrix Λ satisfies the relations

$$\Lambda^2 = -1,$$
$$\Lambda^{-1} = \Lambda^{\mathrm{T}} = -\Lambda.$$ (2.15)

By inverting both sides of Eq. (2.11) and using (2.13), we find that the monodromy matrix possesses the symplectic property as well, i.e.,

$$M_1^{-1} = \Lambda M_1^{\mathrm{T}} \Lambda^{-1}.$$ (2.16)

This relation says that M_1^{-1} and M_1^{T} have the same eigenvalues. Since M_1 and M_1^{T} have the same eigenvalues, it follows that M_1^{-1} and M_1 have the same eigenvalues.

Therefore, *all eigenvalues of M_1 occur in pairs of inverses.* This is a well-known property of the continuum monodromy matrix [3]. The above argument shows that it is also an exact property of the discretized one.

We recall that the original trajectory (x_n, y_n) was periodic, i.e., it satisfies Eqs. (2.3). If we want the neighbor trajectory $(x_n + \delta_n, y_n + \delta y_n)$ to be periodic also, we must have $Z_{N+1} = Z_1$. According to (2.10), this means that Z_1 must be an eigenvector of M_1 for eigenvalue 1. But we actually know another, close-by, periodic solution of Eqs. (2.4), namely that solution in which every (x_n, y_n) has been replaced by (x_{n+1}, y_{n+1}) or, in other words, the identical trajectory with the points relabelled. The Z_1 corresponding to this "neighbor" is

$$Z_1 = \begin{pmatrix} x_2 - x_1 \\ y_2 - y_1 \\ x_1 - x_0 \\ y_1 - y_0 \end{pmatrix}. \tag{2.17}$$

This Z_1 is not infinitesimal and, consequently, the present argument is only approximate. Within this approximation, however, the above Z_1 must be an eigenvector of M_1 for eigenvalue unity. Our numerical work shows that, for small values of ε (for instance $N = 100$ in the case of a relatively simple trajectory, more for complicated ones), the approximation is actually excellent and the monodromy matrix has an eigenvalue which is very close to 1. Therefore, by the theorem of the previous paragraph, it also has a second eigenvalue very close to 1, which is the exact inverse of the first one. We find also that, for both eigenvalues, the eigenvector is very close to (2.17).

The two other eigenvalues of M_1 must have unit product. And the complex conjugate of every eigenvalue must also be an eigenvalue, because M_1 is real. This leads to two possible cases. In one case, which we shall call case S, the eigenvalues are $(e^{+i\alpha}, e^{-i\alpha})$; i.e., they have unit modulus and are complex conjugates. In this case, the trace of the monodromy matrix is

$$\text{Tr } M_1 \simeq 2(1 + \cos \alpha) \tag{2.18}$$

and therefore

$$0 < \text{Tr } M_1 < 4 \qquad \text{(case } S\text{)}. \tag{2.19}$$

In the other case, which we shall call case U, the eigenvalues are real and can be either $(e^{\beta}, e^{-\beta})$ or $(-e^{\beta}, -e^{-\beta})$. The trace of M_1 is then

$$\text{Tr } M_1 \simeq 2(1 \pm \cosh \beta), \tag{2.20}$$

which leads to

$$\text{Tr } M_1 > 4 \qquad \text{or} \qquad \text{Tr } M_1 < 0 \qquad \text{(case } U\text{)}. \tag{2.21}$$

It is well-known [3] that these eigenvalues determine the stability of the periodic trajectory. According to the stability theorem of Liapunov [3], most of the trajectories belonging to case S are stable, except for a set of measure zero corresponding to some values of α which are rational multiples of 2π, and all the trajectories belonging to case U are unstable. Therefore, to simplify matters, we shall refer to those regions in which inequality (2.19) is satisfied as stable regions, and to those regions in which inequality (2.21) is satisfied as unstable regions. It is very nice that one can determine the stability or instability, simply by looking at the trace of the monodromy matrix, without having to solve any eigenvalue equation. This is true only in two dimensions, not in higher dimensionalities.

When M_1 has an eigenvector Z_1 with eigenvalue $e^{\pm i\alpha}$, where $\alpha = 2\pi l/k$, l and k being non-commensurate integers with $l < k$, it is evident that by propagating Z_1 around the trajectory k times one returns with the initial value; i.e., one manufactures a periodic trajectory whose period is k times the period of the original one. Thus, such points are bifurcation points for period k-upling. We actually find the period-multiplied trajectories by following this procedure. These bifurcation points are everywhere dense on the interval (2.19), but we limit ourselves to the simplest values of k, $k = 1$ to 6, for obvious reasons. In particular, we have a period-tripling when $\text{Tr } M_1 = 1$ and a period-quadrupling when $\text{Tr } M_1 = 2$. The period-doubling case, $k = 2$, $\text{Tr } M_1 = 0$, is special because it corresponds to the edge of the interval of stability. At the other end of this interval, we have $\text{Tr } M_1 = 4$, all four eigenvalues equal to 1. This is where one should find the isochronous branchings ("no change of period"), when two distinct families, each with its own pair of eigenvalues equal to 1, coalesce into one. We shall present further discussion of the various types of branchings in Sections 4 and 5.

We note before ending this section that the M-matrix could have been defined in any one of N different ways, depending on the starting point of the varied trajectory. For instance, instead of (2.11), we could have used

$$M_n = U_{n-1} U_{n-2} \cdots U_2 U_1 U_N U_{N-1} \cdots U_{n+1} U_n. \tag{2.22}$$

The matrices M_n and M_1 are different (if $n \neq 1$), but they have the same eigenvalues.

3. NUMERICAL RESULTS

The MARTA potential, Fig. 1, has a minimum at the origin with $V = 0$ and two saddle points at $(x, y) = (\pm\sqrt{3}, 1)$ with $V = \frac{3}{4}$. The periodic families issuing from the small oscillations about the origin in the horizontal (x) and vertical (y) directions are called H and V, respectively. The V family has constant period $(\tau = 2\pi/\sqrt{3})$ since the one-dimensional potential $V(0, y)$ is harmonic. This is not true of $V(x, 0)$ and the H family is non-trivial. The families issuing from the transversal oscillations (in direction of slope $\mp 2/\sqrt{3}$) about the saddle points $(\pm\sqrt{3}, 1)$ are labelled $S_{\pm}$. When a family F undergoes a period n-upling bifurcation, the new

families branching off are labelled *Fna*, *Fnb*, and so on. If the family exhibits other period n-upling bifurcations, they are labelled *Fna'*, *Fnb'*, and so on. When *Fna* undergoes a period m-upling bifurcation, the new families are labelled *Fnama*, *Fnamb*, and so on. In the case of isochronous $(n = 1)$ bifurcation the n is omitted.

The E–τ plots for the H family and its branchings and for the V family and its branchings are shown in Figs. 2 and 3, respectively. The E–τ plot for the S_+ families is shown in Fig. 4. As in Ref. [1], the periodic families which are *rotations* have been marked with the symbol ρ in the E–τ plot; families which are not so marked are *librations*. We use heavy lines or the symbol S to indicate the regions of stability of a family and thin lines or the symbol U to indicate the regions of instability. The points corresponding to the limiting values of Tr M, 4 and zero (Z), are also marked in the E–τ plots. The symbol Z^2 is used when Tr $M = 0$ and $(d\,\mathrm{Tr}\,M)/dE = 0$, $\bar{4}$ is used when Tr $M = 4$ and $dE/d\tau = 0$, and 4^2 when Tr $M = 4$ and $(d\,\mathrm{Tr}\,M)/dE = 0$ (see Fig. 5).

The saddle point families $S_\pm$ are always unstable and, therefore, do not exhibit any period n-upling bifurcations (some values of Tr M are indicated in Fig. 4). As for the H and V families, they exhibit more than one interval of stability: H has 2 intervals and V has several, which get smaller and smaller as energy increases.
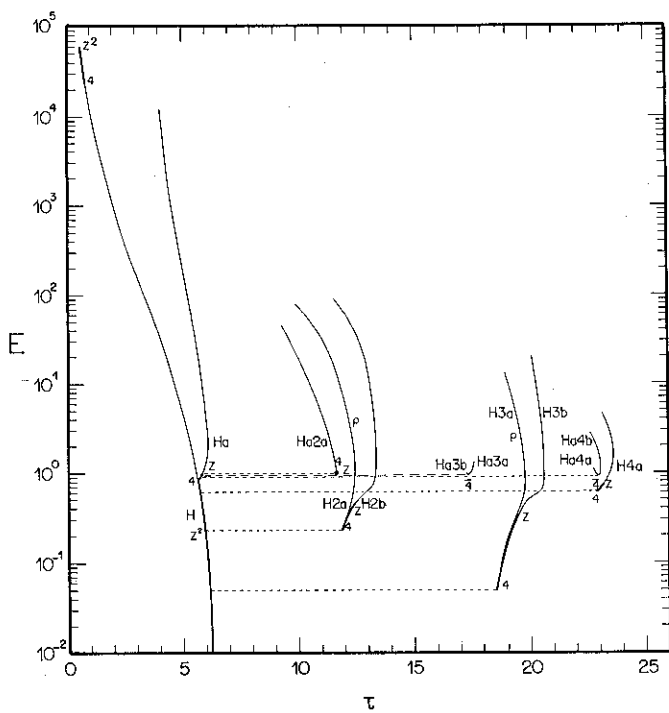
FIG. 2. $E \times \tau$ plot of the horizontal families.
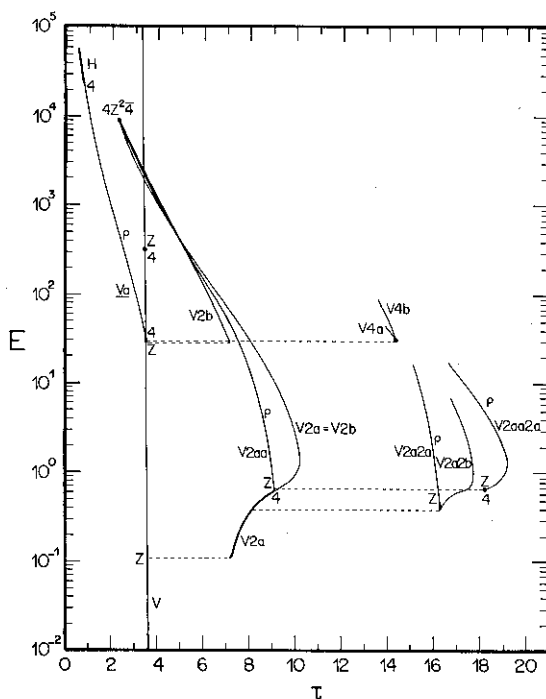
FIG. 3. $E \times \tau$ plot of the vertical families.

In Fig. 3, it is seen that the families $V2a$, $V2b$, and $V2aa$ form a loop showing that $V2a$ and $V2b$ are in fact the same family. This is shown in detail in Fig. 6 where we have intentionally enlarged the width of the cycles to show the topology of the curve. The rotation $V2aa$ acts like a bridge connecting the two stable regions of the libration. The first period tripling of V has a complicated topology shown separately in Fig. 7. We found that the horizontal and vertical families are connected by a rotation, $Va = Hb$, which bifurcates isochronously at both ends, as shown in Fig. 8.

For an integrable system, all families of periodic trajectories branch off one of the two basic families, which are obtained by setting one of the two actions equal to zero. This is not true in a non-integrable system. In fact, in our case, we found families which are isolated on the E–τ plot and do not connect with the horizontal or the vertical families. The E–τ plots for these isolated families have the shape of an eight as shown in Fig. 9 (intentionally enlarged). These families have regions of stability starting (or ending) at the maximum and minimum of the energy. A group of these families is shown in Fig. 10. Note that most of them have a rotation connecting, by isochronous branching, the two regions of stability at the maximum and minimum of the curve. In Fig. 11 we display a sequence of trajectories (projected on the x–y plane) for such a rotation, namely family Fa, which branches

DE AGUIAR ET AL.
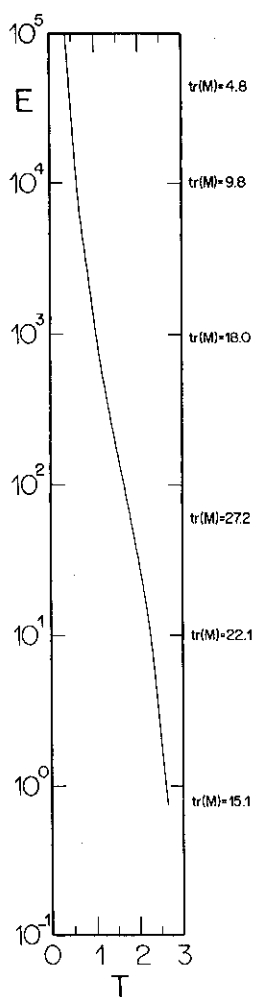
FIG. 4. $E \times \tau$ plot for the saddle point families.
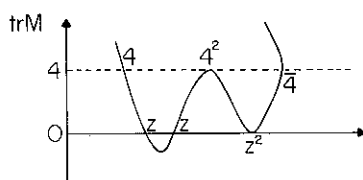
FIG. 5.   Tr $M \times E$, illustrating the points denoted by 4, 4^2, Z, Z^2, and $\bar{4}$.

off the isolated family F. We see in Section 4 that the existence of this isochronous bridge requires at least one symmetry for the original trajectory, either time-reversal or x-reversal symmetry. In other words, the trajectory must be either a libration or an x-symmetric rotation. Figure 12 shows an isolated family of asymmetric rotations which does not have an isochronous bridge.
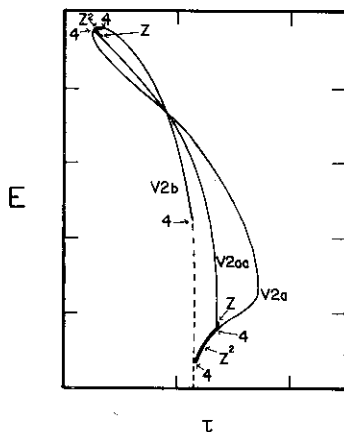
FIG. 6.   Detail of the loops $V2a$, $V2b$, and $V2aa$ (intentionally enlarged out of scale) in Fig. 3.
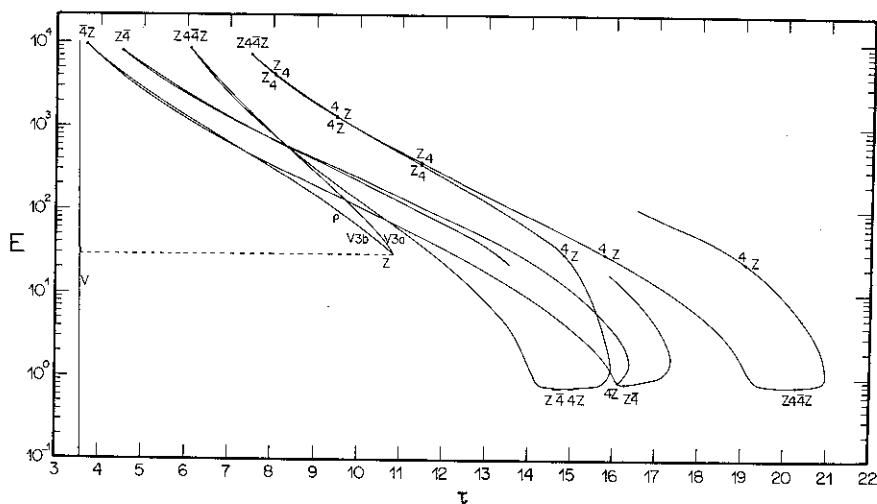
FIG. 7. $E \times \tau$ plot of the first period-tripling families of the V family.

Figure 13 is an x–y plot of some member trajectories of the H family at low energy superimposed over the equipotential lines of $V(x, y)$. Figure 14 is the same thing for some members of the family S_+. In Fig. 15 we show the x–y plot of $V2aa$ branching from $V2a$. In Fig. 16 we show the x–y plot of the trajectories generated at several bifurcation points of the H family. Figure 17 shows a detail of the $E \times \tau$ plot of the period tripled families $Ha3a$, $Ha3b$.
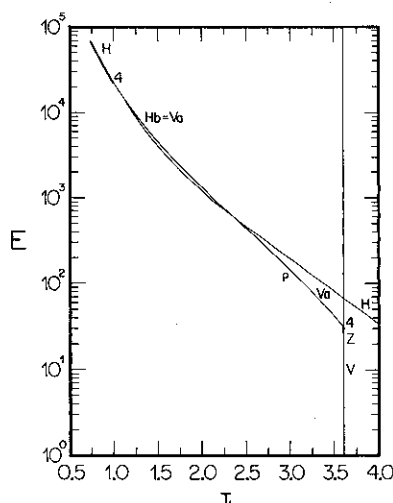
FIG. 8.   Detail of the connection of the horizontal and the vertical families by a rotation, $Va = Hb$.
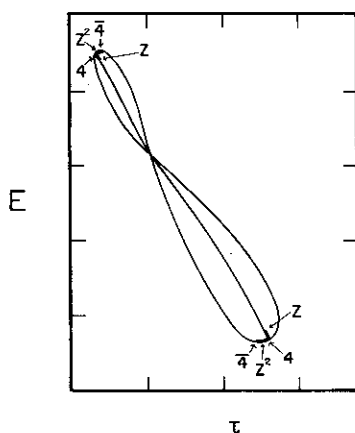
FIG. 9.   Detail of the $E \times \tau$ plot of an isolated symmetric libration family showing the shape of an eight (intentionally enlarged out of scale).
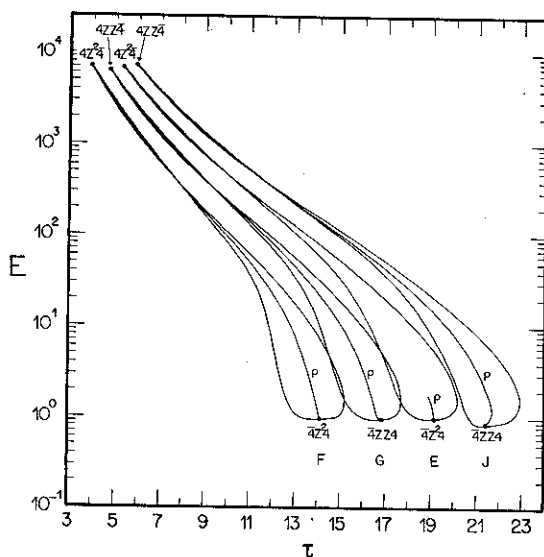
FIG. 10. $E \times \tau$ plot of a group of isolated families.
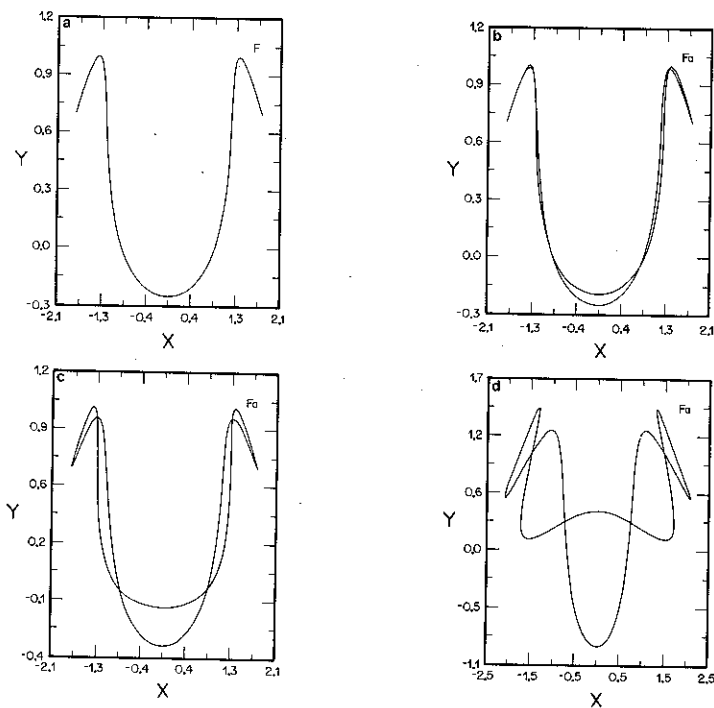
FIG. 11. x–y plot of a member of the irregular family F and a sequence of members of the bifurcated family Fa.

DE AGUIAR ET AL.
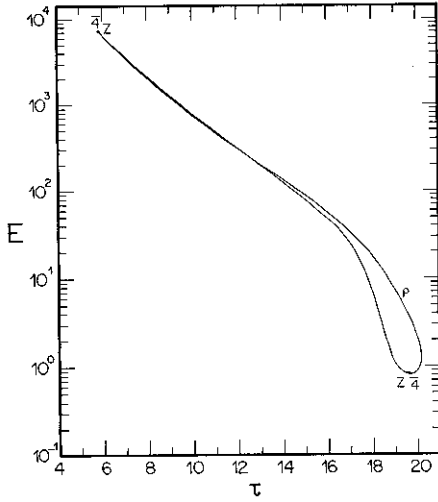
FIG. 12. $E \times \tau$ plot of an isolated family of asymmetric rotations (which does not have an isochronous bridge).
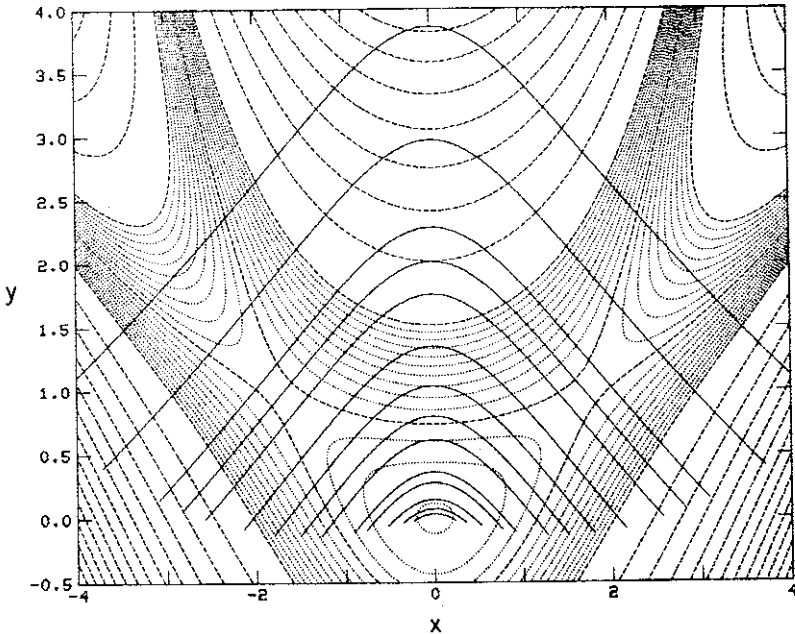
FIG. 13. x–y plot of some trajectories of the H family superimposed over the equipotential lines of $V(x, y)$.
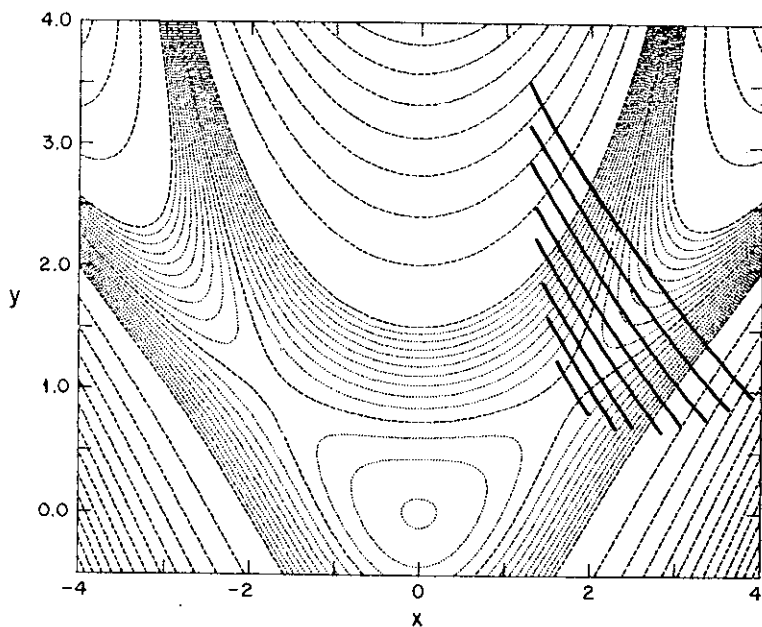
FIG. 14. $x-y$ plot of some trajectories of the S_+ family superimposed over the equipotential lines of $V(x, y)$.
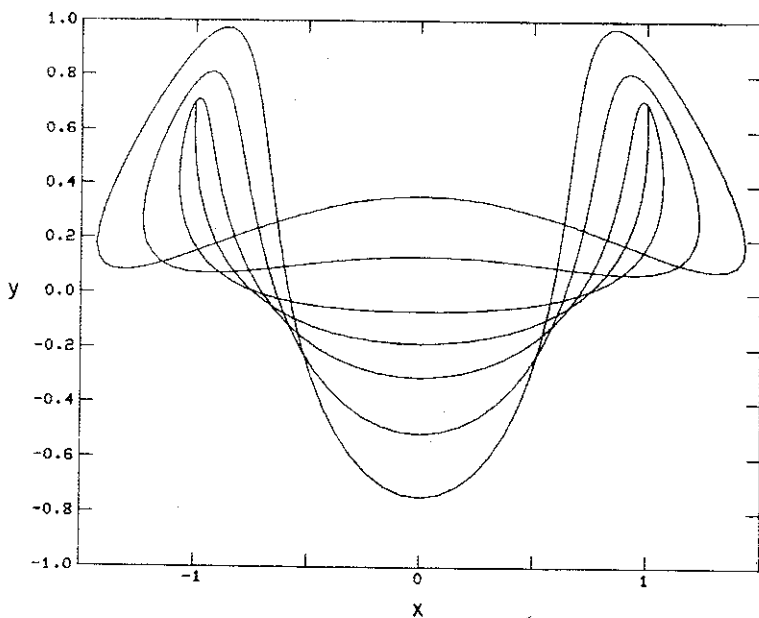
FIG. 15. $x-y$ plots of family $V2aa$ branching from $V2a$.
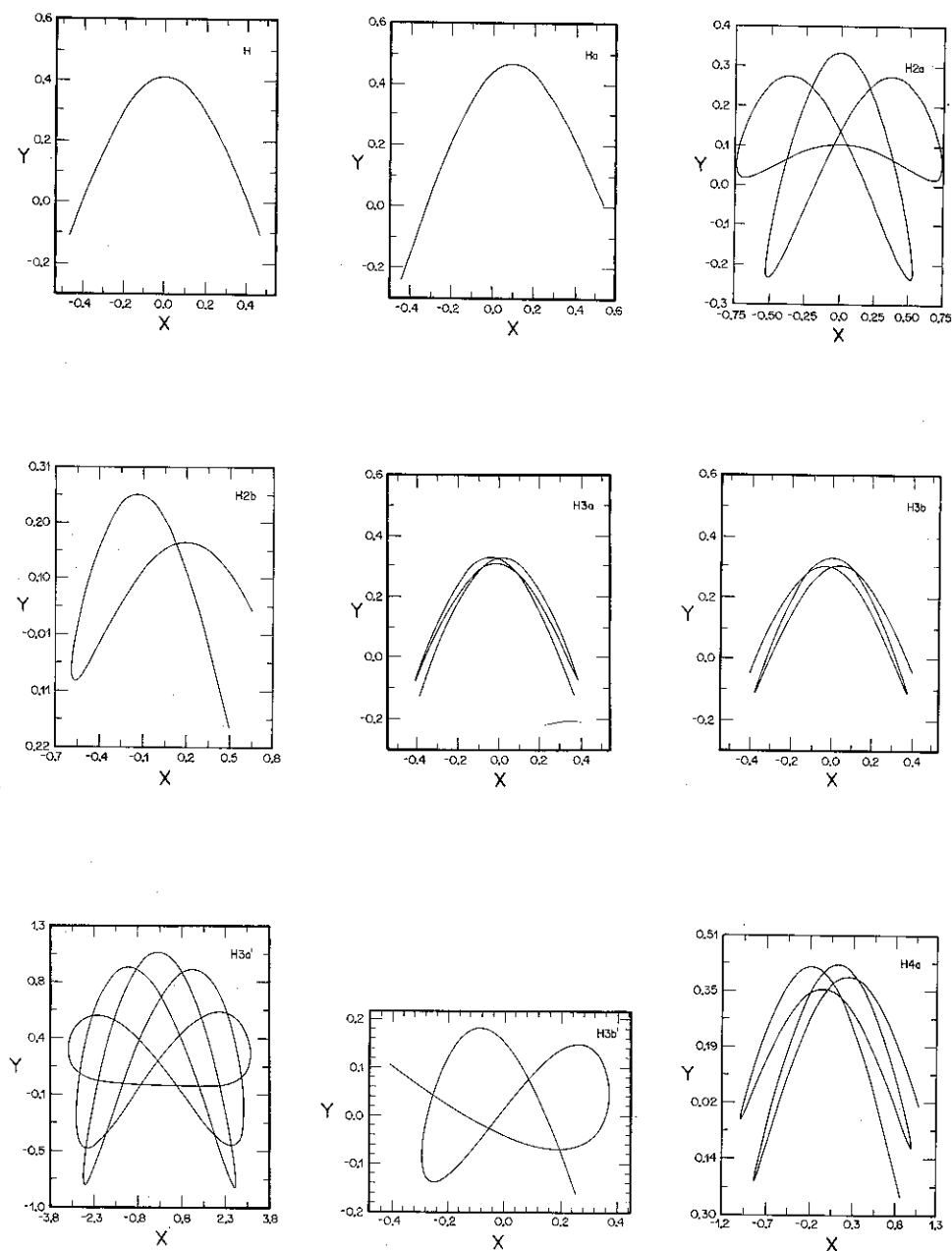
FIG. 16.   x–y plot of member trajectories of the families generated at several bifurcations points of the H family.
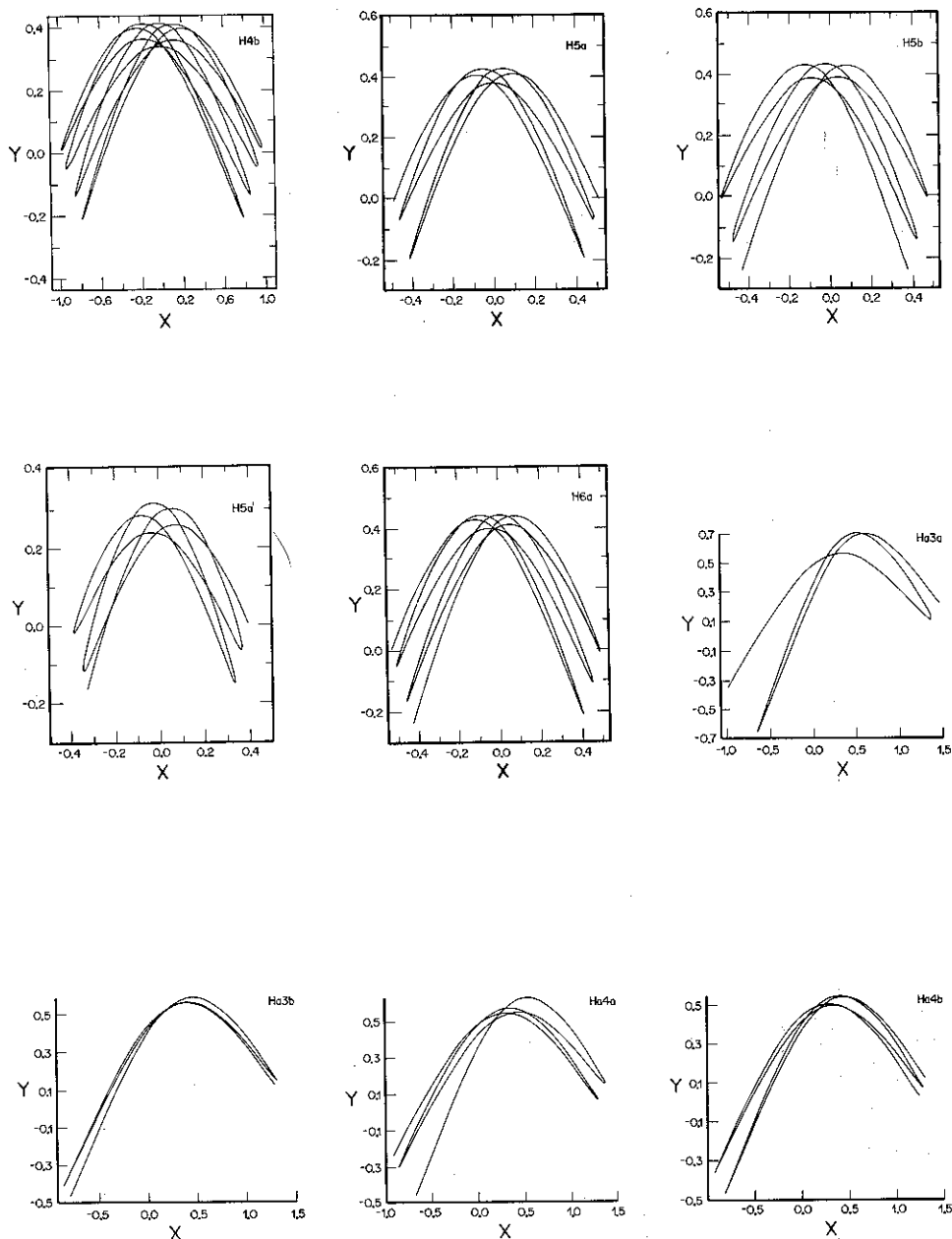
FIGURE 16 (continued)
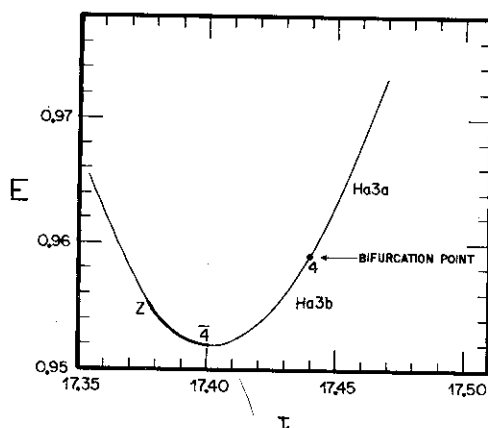
Fig. 17. Detail of the $E \times \tau$ plot of the period tripled families of $Ha3a$ and $Hz3b$.

Our numerical study has shown that the bifurcations of a periodic family can be classified in a few definite categories. These categories remain the same for the other Hamiltonian systems which have been investigated [1, 5, 6]. These findings are summarized in the next section.

4. BIFURCATIONS OF PERIODIC TRAJECTORIES: SUMMARY OF NUMERICAL RESULTS

It is important for this discussion to realize that the periodic trajectories we are considering may have one or both of two different symmetries. One is time-reversal symmetry or t-symmetry: a libration is t-symmetric, a rotation is not. For a time-reversal-invariant Hamiltonian, which is the case here, every periodic solution which is a rotation has a companion solution which is the time-reverse of the first, and which consists of the same x–y trajectory described in the opposite direction. For present purposes, we consider these two rotations as two different periodic trajectories belonging to two different families. A libration, on the other hand, is its own time-reverse and constitutes a single entity from the point of view of t-symmetry.

The other possible symmetry is x-symmetry, which is possible for the present potential because $V(-x, y) = V(x, y)$. A trajectory which is x-symmetric will simply be called "symmetric" from now on, since we have appropriate works already, namely "libration" and "rotation," to describe t-symmetry. Thus we have four kinds of trajectories: symmetric librations (2 symmetries), asymmetric librations and symmetric rotations (1 symmetry), asymmetric rotations (0 symmetry). Again, every asymmetric trajectory has a companion asymmetric trajectory which is the x-reflexion of the first. Thus, an asymmetric rotation always belongs to a quartet.

An analytic study of the bifurcation of periodic trajectories was made by Meyer [7] in the case of Hamiltonian systems without symmetries ("generic case"). Therefore, we had to extend his work to include the two symmetries mentioned above. This extension is presented in Section 5 of this paper. The results agree exactly with our empirical findings. It is interesting that x-symmetry and t-symmetry play exactly the same role in these results, as one might expect from the interchangeability of coordinates and momenta in the canonical formalism; the only thing that matters is the total number of symmetries, N_S, which can be 2, 1, or 0. Bifurcation with preservation of symmetry corresponds to the generic case [7]. Other types of bifurcation result from loss of one symmetry, $\Delta N_S = -1$.

In the following, we describe the topology of the $E \times \tau$ plot in the vicinity of a bifurcation. We also describe the fixed points of the so-called Poincaré map [10] which is used in the above-mentioned analytic study. For a fixed energy, the Poincaré map $\mathscr{P}$ is the map of a plane $x = \text{const.}$ (or $y = \text{const.}$) on itself defined by the consecutive intersections, with $p_x > 0$ ($p_y > 0$), of this plane and the phase space trajectories lying in the vicinity of the periodic trajectory undergoing bifurcation (see Fig. 18). The point where this periodic trajectory intersects the plane is a fixed point of the map $\mathscr{P}$. A period n-upling trajectory corresponds to n fixed points of the map $\mathscr{P}^n$. The Poincaré map is an area preserving map and the Jacobian of its linear approximation is the monodromy matrix. A stable (unstable) periodic trajectory corresponds to an elliptic (hyperbolic) [10] fixed point. (In the neighborhood of an elliptic fixed point the invariant curves of $\mathscr{P}$ are ellipses, and in the neighborhood of a hyperbolic fixed point the invariant curves of $\mathscr{P}$ are hyperboles.)
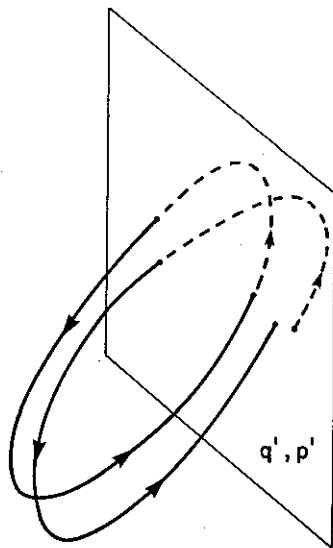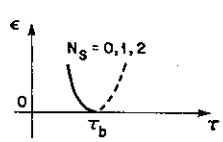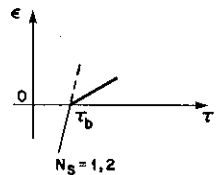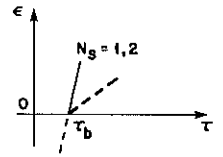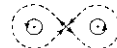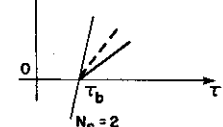

FIG. 18. Illustration of the reduction to one degree of freedom with a coordinate playing the role of time, giving rise to the Poincaré map.

We call E_b the energy of the bifurcation point and τ_b the corresponding period. We set $E = E_b + \varepsilon$ and ε is the parameter which is varied as we cross the bifurcation point. We shall consider only the case when the bifurcated trajectories appear for $\varepsilon > 0$, as the situation for $\varepsilon < 0$ is completely analogous. A full (dashed) line is here used to indicate a stable (unstable) family. Thick lines (full or dashed) indicate that there are two degenerate families branching off the bifurcation point.
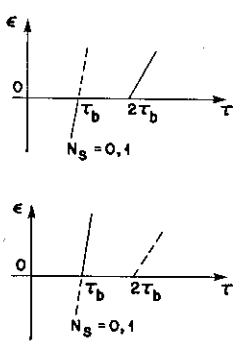
TABLE I

Isochronous Bifurcations
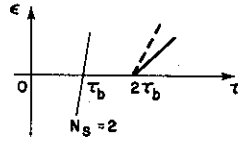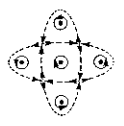
$\epsilon \times \tau$	Fixed points of P	
	$\epsilon \leqslant 0$	$\epsilon > 0$
a Symmetry preserved		
b $\Delta N_S = -1$		
c $\Delta N_S = -1$		

Note. (a) Generic case, the trajectory simply switches from stable to unstable or *vice versa* (it occurs at points denoted by 4 for which Tr $M = 4$ and $dE/d\tau = 0$); (b) bifurcations with loss of one symmetry and change of stability of the bifurcating trajectory (they occur at points denoted by 4); (c) bifurcations with loss of one symmetry with the bifurcating trajectory remaining stable (however, see Remark 1 at the end of Section 4).

In Table I we present the $E \times \tau$ plot in the vicinity of an isochronous bifurcation (Tr $M = 4$) together with the fixed points of $\mathscr{P}$ and its invariant curves in their vicinity. (The arrows indicate the direction of the map flow.) We indicate the number of symmetries N_S of the bifurcating trajectory and the variation ΔN_S. In Tables II to V we present the $E \times \tau$ and the fixed points of $\mathscr{P}^k$ for period k-upling ($k \geqslant 2$) bifurcations.
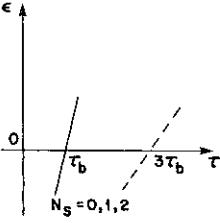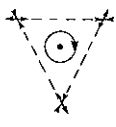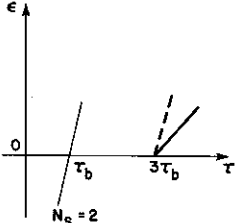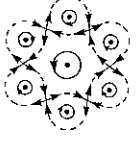
The period k-upling bifurcations of the V family, k odd $\geqslant 3$, are different; therefore, we display them separately in Table VI. The period $2k$-upling bifurcations of the V family are generic, the bifurcated trajectories being symmetric librations (the V family does not have Z^2 or 4^2 branching points).

TABLE II

Period-Doubling Bifurcations

Note. (a) Generic case (symmetry preserving bifurcation occurring at points denoted by Z); (b) bifurcation at Z^2 points, each pair of alternating fixed points corresponding to one periodic trajectory.

TABLE III

Period-Tripling Bifurcations

$\epsilon \times \tau$	Fixed points of P^3		
	$\epsilon < 0$	$\epsilon = 0$	$\epsilon > 0$
a Symmetry preserved			

| b $\Delta N_S = -1$ | | | |

Note. (a) Generic case; (b) bifurcation with loss of one symmetry, each set of alternating fixed points corresponding to one periodic tranjectory.
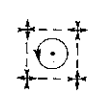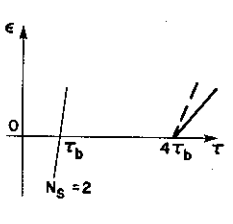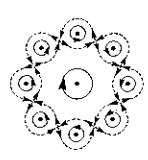
Remarks. 1.   We did not find any 4^2 branchings for MARTA. Some were found into two of the other potentials [1, 5]. However, two of us [14] have demonstrated recently that 4^2 branchings actually do not exist: they consist of two distinct, but very closely spaced, single 4's.

2.   The numerical results do not go beyond period 6-upling.

5. BIFURCATIONS OF SYMMETRIC PERIODIC TRAJECTORIES: ANALYTIC STUDY

The Poincaré map introduced in Section 4 is generated by a reduced Hamiltonian obtained as follows. In the vicinity of a periodic orbit we may

TABLE IV

Period-Quadrupling Bifurcations

$\epsilon \times \tau$	Fixed point of P^4		
	$\epsilon < 0$	$\epsilon = 0$	$\epsilon > 0$
a Symmetry preserved			

Note. (a) Generic case (note that a symmetric libration does not exhibit the generic period-quadrupling); (b) bifurcation with loss of one symmetry, each set of alternating fixed points corresponding to one trajectory.
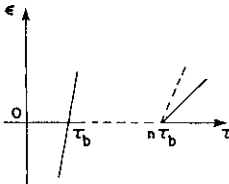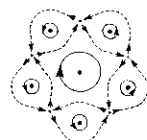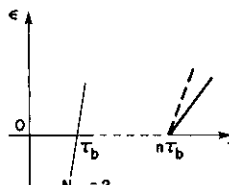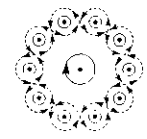
introduce periodic coordinates and transform the original time-independent Hamiltonian with to degrees of freedom into a periodic Hamiltonian with one degree of freedom [11]. The coordinate varying along the trajectory will be called time and its period will be 2π. Using energy conservation,

$$H(x, p_x, y, p_y) = E, \tag{5.1}$$

the reduced Hamiltonian is defined as

$$h(p', q', t) \equiv p_x(E, y, p_y, -x), \tag{5.2}$$

TABLE V

Period k-upling Bifurcation, $k \geqslant 5$

Note. (a) Generic case (note that k even does not exhibit the generic case if the bifurcating trajectory is a symmetric libration); (b) bifurcation with loss of one symmetry, each set of alternating fixed points corresponding to one periodic trajectory.
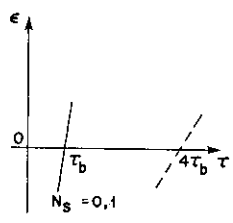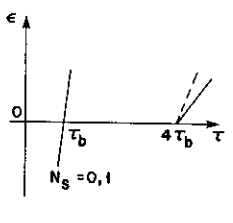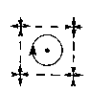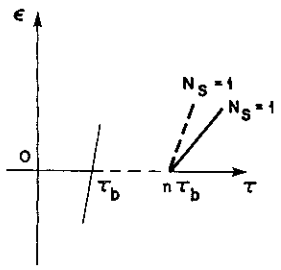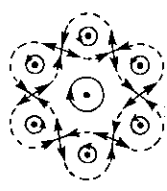
where we have set $q' = y$, $p' = p_y$, and $t = -x$ (see Fig. 18). The action restricted to orbits of energy E in the vicinity of the periodic trajectory is

$$\int (p_x \, dx + p_y \, dy) - \int H \, dt = -\int p_x(-dx) + \int p_y \, dy - Et \qquad (5.3)$$

and its variation restricted to the energy shell gives the following equations of motion

$$\dot{q}' = \frac{\partial h}{\partial p'},$$

$$\dot{p}' = -\frac{\partial h}{\partial q'}. \qquad (5.4)$$

TABLE VI

V Family Period k-upling, $k \geqslant 3$ Odd

$\epsilon \times \tau$	Fixed points of P^n, $n \geqslant 3$ odd	
	$\epsilon \leqslant 0$	$\epsilon > 0$

Note. The bifurcated trajectories have one symmetry (each set of alternating fixed points corresponds to one periodic trajectory).

We have

$$h(q', p', t) = h(q', p', t + 2\pi), \tag{5.5}$$

and the Poincaré map $\mathscr{P}$ is the mapping of the (q', p') plane on itself defined as

$$\mathscr{P}: (q'(t), p'(t)) \to (q'(t+2\pi), p'(t+2\pi)), \tag{5.6}$$

with $q'(t), p'(t)$ solutions of (5.4) (see Fig. 18). It is an area preserving map possessing all the symmetries of the reduced Hamiltonian. And the Jacobian of its linear approximation is the monodromy matrix.

Of course, we could have defined the reduced Hamiltonian $p_y(E, x, p_x, -y)$. The choice of a particular reduced Hamiltonian is in general a matter of convenience. In the case of the vertical harmonic oscillation (family V) we must use the reduced Hamiltonian p_y as this family lies on the (y, p_y) plane and therefore cannot cut a (y, p_y) plane transversally.

The intersection of the periodic trajectory with the plane (q', p') is a fixed point of $\mathscr{P}^k$, $k \geqslant 1$. At period k-upling bifurcation points (E_b, τ_b) new fixed points of $\mathscr{P}^k$ will appear corresponding to the bifurcated trajectories.

It is convenient to change from coordinates (q', p') to coordinates (q, p) so that

for any given periodic family the origin will be the fixed point corresponding to the trajectory of energy E_b and period τ_b. In terms of (q, p) the reduced Hamiltonian (5.2) can be written [12] as

$$h(q, p, t) = h_0 + \frac{\omega}{2}(p^2 + q^2) + \sum_{m=-\infty}^{\infty} \sum_{j_1+j_2=3}^{\infty} K_{j_1 j_2 m} p^{j_1} q^{j_2} e^{imt}, \qquad (5.7)$$

where $h_0 = $ constant is the reduced energy of the fixed point trajectory and $\omega = \alpha/2\pi$ (see (2.18)) is a rational number as discussed in the end of Section 2.

The method of Meyer [7] consists of obtaining the fixed points of $\mathscr{P}^k$ at a period k-upling bifurcation point using in its vicinity the lowest order terms of the expansion of $\mathscr{P}$. For $k \geqslant 3$, the normal form [12] expansion for $\mathscr{P}$ is used, while for $k = 1, 2$ he uses the expansion in powers of p and q. We use the same technique as Meyer [7], imposing the existing reflexion symmetries. If R is a reflexion symmetry (i.e., $R^2 = 1$) of $\mathscr{P}$, then

$$\mathscr{P}^{-1} = R\mathscr{P}R. \qquad (5.8)$$

This is illustrated in Fig. 19.

If a canonical transformation U is performed

$$(p, q) \rightarrow (\tilde{p}, \tilde{q}),$$

the transformed Poincaré map is

$$\tilde{\mathscr{P}} = U^{-1}\mathscr{P}U,$$

which will have the generalized reflexion symmetry

$$\tilde{R} = U^{-1}RU.$$

Therefore, canonical transformations conserve the number of reflexion symmetries of the Poincaré map. Moreover, $\tilde{R} \rightarrow R$ at the fixed point.
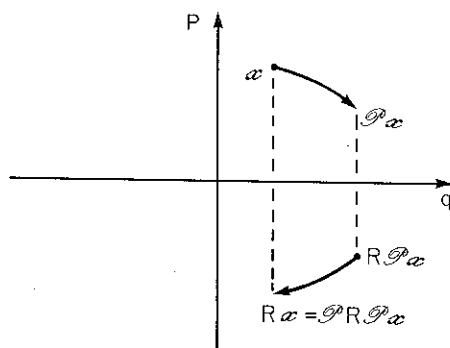
Fig. 19. Illustrating the effect of a reflexing symmetry R on the map $\mathscr{P}$.

We shall first consider the case of a single reflexion symmetry and then the case of two reflexion symmetries. In the end we consider the period k-upling bifurcations, $k \geqslant 3$, of the vertical (harmonic) family which is a special case.

Given the map

$$\begin{pmatrix} q_1 \\ p_1 \end{pmatrix} = \mathcal{P} \begin{pmatrix} q_0 \\ p_0 \end{pmatrix}, \tag{5.9}$$

if we take as reflexion symmetry

$$R = \begin{pmatrix} 1 & 0 \\ 0 & -1 \end{pmatrix},$$

the invariance condition (5.8) can be written as

$$\mathcal{P} \begin{pmatrix} q_1 \\ -p_1 \end{pmatrix} = \begin{pmatrix} q_0 \\ -p_0 \end{pmatrix}. \tag{5.10}$$

The area preserving condition for (5.9) is

$$\frac{\partial q_1}{\partial q_0} \frac{\partial p_1}{\partial p_0} - \frac{\partial q_1}{\partial p_0} \frac{\partial p_1}{\partial q_0} = 1. \tag{5.11}$$

The linear part of $\mathcal{P}$ will be denoted by $\mathcal{P}_l$ (its Jacobian is the monodromy matrix [3]) and we now prove

PROPOSITION 5.1.   *Let $\mathcal{P}$ be a Poincaré map possessing one reflexion symmetry. If $\mathcal{P}_l$ has only unit eigenvalues, the bifurcations are of types* (a) *and* (b) *in Table I.*

Proof.   Up to second order, (5.9) can be written as

$$q_1 \simeq q_0 + A p_0 + \varepsilon(a_0 + a_1 q_0 + a_2 p_0) + a_{11} q_0^2 + a_{12} p_0 q_0 + a_{22} p_0^2,$$
$$p_1 \simeq p_0 + B q_0 + \varepsilon(b_0 + b_1 q_0 + b_2 p_0) + b_{11} q_0^2 + b_{12} p_0 q_0 + b_{22} p_0^2, \tag{5.12}$$

where ε is the energy parameter introduced in Section 4 ($E = E_b + \varepsilon$).

Area preservation condition (5.11) implies that $AB = 0$. This will be satisfied if either (i) $A = 0$ of (ii) $B = 0$. As the parameter ε is varied, case (ii) gives rise to the generic isochronous bifurcation (4) and (i) to bifurcations of type (b) in Table I.

Case (i). $A = 0$, $B \neq 0$. In this case, the symmetry condition (5.10) together with area preservation implies that $a_1 = a_2/2 - a_{12}b_0/2$, $a_{11} = -b_{22} = a_{12}/2$, $a_{22} = b_{12} = a_0 = 0$. Without any loss of generality we set $B = 1$ and $a_2 = 1$ and the map (5.12) is then given by

$$q_1 = q_0 + \frac{\varepsilon}{2} \left[(1 + b_0 a_{12}) q_0 + 2 p_0 \right] + a_{12} q_0^2 + 2 a_{12} q_0 p_0 + O(\varepsilon^2),$$

$$p_1 = p_0 + q_0 + b_{11} q_0^2 - \frac{a_{12}}{2} p_0^2 + \frac{\varepsilon}{2} \left[2 b_0 + 2 b_1 q_0 + (1 - b_0 a_{12}) p_0 \right] + O(\varepsilon^2). \tag{5.13}$$

We look for non-trivial fixed points $(q(\varepsilon), p(\varepsilon))$ of $\mathscr{P}$ such that

$$(q(\varepsilon), p(\varepsilon)) \xrightarrow{\varepsilon \to 0} (0, 0).$$

So we make in (5.13) the following substitution

$$p_i = \sqrt{\varepsilon}\, t_i,$$
$$q_i = \varepsilon r_i, \qquad i = 0, 1, \tag{5.14}$$

obtaining

$$r_1 = r_0 + \sqrt{\varepsilon}(a_{12} r_0 t_0 + a_{33} t_0^3 + t_0) + O(\varepsilon),$$
$$t_1 = t_0 + \sqrt{\varepsilon}\left(r_0 - \frac{a_{12}}{2} t_0^2 + b_0\right) + O(\varepsilon). \tag{5.15}$$

In the above expression the term in p_0^3 has been included because it is of order $\sqrt{\varepsilon}$. Defining the functions

$$f(r, t, \varepsilon) = \frac{r_1 - r_0}{\sqrt{\varepsilon}},$$
$$g(r, t, \varepsilon) = \frac{t_1 - t_0}{\sqrt{\varepsilon}}, \tag{5.16}$$

the fixed points of (5.15) are solutions of

$$f(r, t, \varepsilon) = 0,$$
$$g(r, t, \varepsilon) = 0.$$

The implicit function theorem [3] applied to functions f and g guarantees the existence of functions $r(\varepsilon)$ and $t(\varepsilon)$ such that

$$f(r(\varepsilon), t(\varepsilon), \varepsilon) = 0,$$
$$g(r(\varepsilon), t(\varepsilon), \varepsilon) = 0,$$

with

$$r(0) = -b_0,$$
$$t(0) = 0, \tag{5.17}$$

or

$$r(0) = (a_{12} - b_0(a_{12}^2 + 2\eta))/2\eta,$$
$$t(0) = \pm(\xi/\eta)^{1/2}, \tag{5.18}$$

where

$$\eta = -(a_{12}^2 + 2a_{33})/2,$$
$$\xi = 1 - a_{12}b_0.$$

Thus, $(r(0), t(0))$ given by (5.17) and (5.18) are the fixed points of (5.15) with (5.17) corresponding to the bifurcating trajectory and (5.18) to the bifurcated trajectories. Correspondingly, the fixed points of (5.13) are

$$q(\varepsilon) = -b_0\varepsilon,$$
$$p(\varepsilon) = 0,$$
(5.19)

and

$$q(\varepsilon) = \varepsilon(a_{12} - b_0(a_{12}^2 + 2\eta))/2\eta,$$
$$p(\varepsilon) = \pm(\varepsilon\xi/\eta)^{1/2}.$$
(5.20)

The eigenvalues of the Jacobian of (5.13) calculated at the fixed point (5.19) are

$$\lambda = 1 \pm \sqrt{\xi\varepsilon} + O(\varepsilon)$$
(5.21)

and at the fixed points (5.20) are

$$\bar{\lambda} = 1 \pm \sqrt{-2\xi\varepsilon} + O(\varepsilon).$$
(5.22)

Now, assuming $\xi > 0$, if $\eta > 0$, for $\varepsilon \leqslant 0$ only the fixed point (5.19) exists and it is stable (see (5.21)); for $\varepsilon > 0$ there exist the fixed point (5.19) now unstable (see (5.21)) and the two fixed points (5.20) that are stable (see (5.22)).

For $\xi < 0$, if $\eta < 0$, for $\varepsilon \leqslant 0$ only the fixed point (5.19) exists and it is unstable; for $\varepsilon > 0$ there exist the fixed point (5.19), stable, and the fixed points (5.20), unstable.

These bifurcations correspond to case (b) presented in Table I and the second part of the proposition is proved.

Remark. For $\xi > 0$, $\eta < 0$, and $\xi < 0$, $\eta > 0$, we obtain the same type of bifurcation with the bifurcated trajectories existing for $\varepsilon < 0$.

Case (ii). $B = 0$, $A \neq 0$. In this case, the reflexion symmetry condition (5.10) together with area preservation imply that $b_1 = 2a_1 - 2a_0(a_{12} - a_{11})$, $b_2 = b_1 - a_1$, $b_{11} = b_{12} = 2a_{11}$, $a_{12} = 4a_{22}$, $b_{22} = a_{11} - 2a_{22}$, and $a_0 = b_0/2$. Without any loss of generality, we set $A = 1$ and $a_1 = 1$ and the map (5.12) is given by

$$q_1 = q_0 + p_0 + \varepsilon(q_0 + a_2 p_0 + b_0/2) + 4a_{22}p_0q_0 + a_{11}q_0^2 + a_{22}p_0^2 + O(\varepsilon^2),$$
$$p_1 = p_0 + \varepsilon(b_1q_0 + b_2 p_0 + b_0) + 2a_{11}q_0(p_0 + q_0) + (a_{11} - 2a_{22})p_0^2 + O(\varepsilon^2).$$
(5.23)

We now make the substitution

$$
\begin{aligned}
q_i &= \sqrt{\varepsilon}\, r_i, \\
p_i &= \sqrt{\varepsilon}\, t_i, \qquad i = 0, 1
\end{aligned}
\tag{5.24}
$$

obtaining

$$
\begin{aligned}
r_1 - r_0 &= t_0 + \sqrt{\varepsilon}\left(\frac{b_0}{2} + 4a_{22}r_0 t_0 + a_{11}r_0^2 + a_{22}t_0^2\right) + O(\varepsilon), \\
t_1 - t_0 &= \sqrt{\varepsilon}(b_0 + 2a_{11}r_0 t_0 + 2a_{11}r_0^2 + (a_{11} - 2a_{22})\, t_0^2) + O(\varepsilon).
\end{aligned}
\tag{5.25}
$$

From the implicit function theorem [3] the fixed points of (5.25) are

$$
r_{\pm}(0) = \pm\left(-\frac{b_0}{2a_{11}}\right)^{1/2},
$$

$$
t(0) = 0.
$$

Correspondingly, the fixed points of (5.23) are (see (5.24))

$$
q_{\pm}(\varepsilon) = \pm\left(-\frac{\varepsilon b_0}{2a_{11}}\right)^{1/2},
$$

$$
p(\varepsilon) = 0.
\tag{5.26}
$$

The eigenvalues of the Jacobian of (5.23) at $(q_+(\varepsilon), 0)$ are

$$
\lambda_+ = 1 \pm 2\left(-\frac{\varepsilon a_{11} b_0}{2}\right)^{1/4},
\tag{5.27}
$$

and at $(q_-(\varepsilon), 0)$ are

$$
\lambda_- = 1 \pm i2\left(-\frac{\varepsilon a_{11} b_0}{2}\right)^{1/4}.
\tag{5.28}
$$

Thus, if $a_{11}b_0 < 0$ $(a_{11}b_0 > 0)$ no fixed point exists for $\varepsilon < 0$ $(\varepsilon > 0)$ while for $\varepsilon > 0$ $(\varepsilon < 0)$ there exist two fixed points: one unstable (5.27) and one stable (5.28). The case $a_{11}b_0 < 0$ corresponds to a minimum in the $\varepsilon \times \tau$ plot at $\varepsilon = 0$ and $a_{11}b_0 > 0$ corresponds to a maximum. This is the generic type of bifurcation $(\bar{4})$ corresponding to case (a) in Table I. And the proof of Proposition 5.1 is completed. ∎

We now consider the period-doubling bifurcation. In fact, if the bifurcating trajectory has only one reflexion symmetry, the generic type of bifurcation is obtained. This is the content of

PROPOSITION 5.2. *Let $\mathscr{P}$ be a Poincaré map having one reflexion symmetry. If $\mathscr{P}_i$*

has eigenvalues -1 *the bifurcations are of type* (a) *presented in Table II (generic or symmetry preserving).*

Proof. Up to second order, the map $\mathscr{P}$ is given by

$$
\begin{aligned}
q_1 &= -q_0 + Ap_0 + \varepsilon(a_0 + a_1 q_0 + a_2 p_0) + a_{11} q_0^2 + a_{12} q_0 p_0 + a_{22} p_0^2 + \cdots \\
p_1 &= -p_0 + Bq_0 + \varepsilon(b_0 + b_1 q_0 + b_2 p_0) + b_{11} q_0^2 + b_{12} q_0 p_0 + b_{22} p_0^2 + \cdots.
\end{aligned}
\tag{5.29}
$$

Again, area preservation implies $A \cdot B = 0$. We shall consider only case $A = 0$ as $B = 0$ gives the same results.

The symmetry condition (5.10) together with area preservation imply $b_0 = -a_0/2$, $b_2 = -a_1 - a_2$, $b_{11} = (a_{11} + a_{12})/2$, $b_{12} = 2a_{11} - a_{12}$, $b_{22} = a_{12}/2$, $a_{22} = -a_{12}$, and $a_1 = -a_2/2 - a_0(a_{11} + a_{12}/4)$. Without loss of generality, we choose $a_2 = B = 1$ and (5.29) reduces to

$$
q_1 = -q_0 + \varepsilon(a_0 + a_1 q_0 + p_0) + a_{11} q_0^2 + a_{12} q_0 p_0 - a_{12} p_0^2,
$$

$$
p_1 = -p_0 + q_0 + \varepsilon\left[-\frac{a_0}{2} + b_1 q_0 - (1 + a_1) p_0 \right]
$$

$$
+ (2a_{11} + a_{12})\frac{q_0^2}{4} - (a_{12} + 2a_{11}) q_0 p_0 + a_{12}\frac{p_0^2}{2}.
\tag{5.30}
$$

Making the substitution

$$
\begin{aligned}
q_i &= \varepsilon r_i, \\
p_i &= \sqrt{\varepsilon}\, t_i, \qquad i = 0, 1,
\end{aligned}
\tag{5.31}
$$

we obtain

$$
\begin{aligned}
r_1 &= -r_0 + (a_0 - a_{12} t_0^2) + \sqrt{\varepsilon}\, (t_0 + a_{12} r_0 t_0 + a_{33} t_0^3) + O(\varepsilon), \\
t_1 &= -t_0 + \sqrt{\varepsilon}\left(r_0 + \frac{a_{12}}{2} t_0^2 - \frac{a_0}{2} \right) + O(\varepsilon).
\end{aligned}
\tag{5.32}
$$

And the map

$$
\begin{pmatrix} r_2 \\ r_2 \end{pmatrix} = \mathscr{P}^2 \begin{pmatrix} r_0 \\ r_0 \end{pmatrix}
$$

is then given by

$$
\begin{aligned}
r_2 &= r_0 - 2\sqrt{\varepsilon}\, t_0(1 + a_0 a_{12} - a_{12} r_0 + t_0^2(a_{33} - a_{12}^2)) + O(\varepsilon), \\
t_2 &= t_0 - 2\sqrt{\varepsilon}\left(r_0 + \frac{a_{12}}{2} t_0^2 - \frac{a_0}{2} \right) + O(\varepsilon).
\end{aligned}
\tag{5.33}
$$

From the implicit functions theorem [3] the fixed points of $\mathscr{P}^2$ (5.33) are

$$r(0) = \frac{a_0}{2},$$
$$t(0) = 0, \tag{5.34}$$

and

$$r(0) = [a_0(a_{33} - a_{12}^2) + a_{12}]/\delta,$$
$$t(0) = \pm(-2\zeta/\delta)^{1/2}, \tag{5.35}$$

while

$$\delta \equiv 2a_{33} - a_{12}^2,$$

$$\zeta \equiv 1 + a_{12}\frac{a_0}{2}.$$

The fixed point given by (5.34) is also a fixed point of (5.32); therefore it corresponds to a periodic trajectory that was half the period of the trajectory corresponding to the fixed points (5.35).

The eigenvalues of the Jacobian of (5.32), calculated at the fixed point (5.34), are

$$\lambda = -1 \pm (\zeta\varepsilon)^{1/2} + O(\varepsilon), \tag{5.36}$$

and the eigenvalues of the Jacobian of (5.33), calculated at the fixed points (5.35), are

$$\bar{\lambda} = 1 \pm 2(-2\zeta\varepsilon)^{1/2} + O(\varepsilon). \tag{5.37}$$

Thus, if $\zeta > 0$ ($\zeta < 0$) the fixed point (5.34) will switch from stable to unstable as ε varies from negative (positive) to positive (negative) values (see (5.36)). Moreover, if $\delta\zeta < 0$ the fixed points (5.35) will exist only for $\varepsilon > 0$ (see (5.31)) and are stable if $\zeta > 0$ and unstable if $\zeta < 0$. This is the generic period-doubling bifurcation corresponding to cases (a) in Table II. And Proposition 5.2 is demonstrated. ∎

Remark. If $\delta\zeta > 0$ we obtain the same kind of bifurcation with the period-doubled solution existing only for $\varepsilon < 0$.

In order to examine the period k-upling bifurcations, $k \geqslant 3$, we must express the reduced Hamiltonian [5.7] in its normal form [12, 13]. This is achived by making successive time-dependent canonical transformations which eliminate the time dependence of (5.7) up to an order N. The period k-upling bifurcations occur at rational values of ω; therefore we must use the resonant form. Introducing the variables

$$J = \frac{p^2 + q^2}{2},$$

$$\vartheta = \tan^{-1}\frac{p}{q}, \tag{5.38}$$

and writing

$$\omega = \frac{l}{k} + \varepsilon, \qquad l \text{ and } k \text{ non-commensurate integers,} \qquad (5.39)$$

the resonant normal form [12, 13] of (5.7) is obtained from the resonance condition $(l/k)(j_1 - j_2) = m$ (see Appendix). The result is

$$h(J, \vartheta, t) = \varepsilon J + \sum_{j=2}^{k/2} C_j J^j + \alpha J^{k/2} \sin(k\vartheta) + b J^{k/2} \cos(k\vartheta) + \cdots, \qquad (5.40)$$

the time dependence lying in higher order terms (we have set $h_0 = 0$).

The equations of motion, up to order $k/2$, are

$$\dot{J} = -\frac{\partial h}{\partial \vartheta} = akJ^{k/2} \cos(k\vartheta) + bkJ^{k/2} \sin(k\vartheta),$$

$$\dot{\vartheta} = \frac{\partial h}{\partial J} = \varepsilon + \sum_{j=2}^{k/2} C_j j J^{j-1} + a\frac{k}{2} J^{(k/2)-1} \sin(k\vartheta) + b\frac{k}{2} K^{(k/2)-1} \cos(k\vartheta). \qquad (5.41)$$

And the map,

$$\begin{pmatrix} J_1 \\ \vartheta_1 \end{pmatrix} = \mathscr{P} \begin{pmatrix} J_0 \\ \vartheta_0 \end{pmatrix}, \qquad (5.42)$$

is obtained by integrating (5.41) from 0 to 2π in the approximation $J \simeq J_0$, $\vartheta \simeq \vartheta_0$:

$$J_1 = J_0 - 2\pi k a J_0^{k/2} \cos(k\vartheta_0) + 2\pi k b J_0^{k/2} \sin(k\vartheta_0),$$

$$\vartheta_1 = \vartheta_0 + 2\pi\varepsilon + \sum_{j=1}^{(k/2)-1} 2\pi(j+1) C_j J_0^j + \pi k a J_0^{(k/2)-1} \sin(k\vartheta_0) + \pi k b J_0^{(k/2)-1} \cos(k\vartheta_0). \qquad (5.43)$$

We now impose one reflexion symmetry on the map. In the variables (J, ϑ) the reflexion symmetry condition (5.10) becomes (see (5.38))

$$\mathscr{P} \begin{pmatrix} J_1 \\ -\vartheta_1 \end{pmatrix} = \begin{pmatrix} J_0 \\ -\vartheta_0 \end{pmatrix}, \qquad (5.44)$$

which imposed on (5.43) gives $a = 0$ so that (5.43) reduces to

$$J_1 = J_0 + 2\pi k b J_0^{k/2} \sin(k\vartheta_0),$$

$$\vartheta_0 = \vartheta_0 + 2\pi\varepsilon + \sum_{j=1}^{(k/2)-1} 2\pi(j+1) C_j J_0^j + \pi k b J_0^{(k/2)-1} \cos(k\vartheta_0). \qquad (5.45)$$

So now we state

PROPOSITION 5.3.   *Let $\mathscr{P}$ be a Poincaré map having one reflexion symmetry. If its linear approximation $\mathscr{P}_l$ has eigenvalues $e^{\pm 2\pi i l/k}$, l and k noncommensurate integers,*

$l < k$ and $k \geqslant 3$, then it exhibits period k-upling bifurcation of generic type corresponding to cases (a) in Tables III, IV, and V.

Proof. We shall omit it because it follows the proof of Proposition 5.4 given below for the case of two reflexion symmetries. ∎

We now consider the case of two reflexion symmetries, i.e., the bifurcations of symmetric librations.

Remark. We have not obtained the fixed points of the isochronous and period-doubling bifurcations when the trajectory is a *symmetric libration.* In this case, the isochronous bifurcation points are of the types labelled by 4, $\bar{4}$, and 4^2 in the $E \times \tau$ plots, while the period-doubling bifurcation points are of type Z^2 (see Tables I and II). These bifurcations have been investigated by two of us and the results will appear in a forthcoming paper [14].

We shall then analyze the period k-upling bifurcations, $k \geqslant 3$, of symmetric librations. For the reduced Hamiltonian (5.7), the symmetry $x \to -x$ is imposed by replacing m by $2m$ since this symmetry corresponds to invariance of $h(q, p, t)$ when $t \to t + \pi$:

$$h(q, p, t) = \omega \left(\frac{p^2 + q^2}{2} \right) + \sum_{m = -\infty}^{\infty} \sum_{j_1 + j_2 = 3}^{\infty} K_{j_1 j_2 m} p^{j_2} q^{j_2} e^{i2mt}. \tag{5.46}$$

Now, the resonant normal form of (5.46) depends on k being even or odd as the resonance condition is $(l/k)(j_1 - j_2) = 2m$.

If k is *odd*, the lowest order normal form expansion for the reduced Hamiltonian is

$$h(J, \vartheta, t) = \varepsilon J + \sum_{j=2}^{k/2} C_j J^j + b J^{k/2} \cos(k\vartheta) + \cdots \tag{5.47}$$

or

$$h(J, \vartheta, t) = \varepsilon J + \sum_{j=2}^{k} C_j J^j + b J^k \cos(2k\vartheta) + \cdots . \tag{5.48}$$

If k is *even* only form (5.48) is possible.

The map (5.42) is obtained as previously, by integrating the equations of motion in the approximation $J \simeq J_0$, $\vartheta \simeq \vartheta_0$. The reduced Hamiltonian given by (5.47), valid only for k odd, will produce the map given by (5.45) possessing one reflexion symmetry. And the reduced Hamiltonian given by (5.48) leads to the map (valid for k *even* or *odd*)

$$J_1 = J_0 + 2\pi k b J_0^k \sin(2k\vartheta_0),$$

$$\vartheta_1 = \vartheta_0 + 2\pi\varepsilon + \sum_{j=1}^{k-1} 2\pi(j+1) C_j J_0^j + \pi k b J_0^{k-1} \cos(2k\vartheta_0). \tag{5.49}$$

We shall now prove

PROPOSITION 5.4. *Let $\mathscr{P}$ given by* (5.42) *be a Poincaré map possessing two reflexion symmetries (corresponding to a symmetric libration). If the eigenvalues of the monodromy matrix are given by* $e^{\pm 2\pi i l/k}$, $k \geqslant 3$, $l < k$ *(l and k non-commensurate integers), then it exhibits period k-upling bifurcations. If k is even it is of type* (b) *in Table V and if k is odd it may be of either type* (a) *(generic case) or type* (b) *of Tables III and V.*

Proof. If k is odd, one of the possible lowest order normal form expressions for the map is (5.45); therefore, from Proposition 5.3 it follows that the bifurcations are of the generic type (case (a) in Tables III and V). In the case of expansion (5.49) (which is valid for k *even* or *odd*) in order to find the non-trivial fixed points of $\mathscr{P}^k$ we make the substitution

$$J = R\varepsilon \tag{5.50}$$

so that

$$
\begin{aligned}
R_1 - R_0 &= 2\pi k b \varepsilon^{k-1} R_0^k \sin(2k\vartheta_0) + O(\varepsilon^k), \\
\vartheta_1 - \vartheta_0 &= 2\pi\varepsilon(1 + 2C_1 R_0) + O(\varepsilon^2),
\end{aligned}
\tag{5.51}
$$

and

$$
\begin{aligned}
R_k - R_0 &= 2\pi k^2 b \varepsilon^{k-1} R_0^k \sin(2k\vartheta_0) + O(\varepsilon^k), \\
\vartheta_k - \vartheta_0 &= 2\pi\varepsilon k(1 + 2C_1 R_0) + O(\varepsilon^2).
\end{aligned}
\tag{5.52}
$$

And from the implicit function theorem, the fixed points of $\mathscr{P}_k$ (5.52) are

$$R(0) = -\frac{1}{2C_1},$$

$$\vartheta_{2n}^{(+)} = \frac{2n\pi}{k},$$

$$\vartheta_{2n-1}^{(+)} = (2n-1)\frac{\pi}{k}, \tag{5.53}$$

$$\vartheta_{2n}^{(-)} = \left(2n + \frac{1}{2}\right)\frac{\pi}{k},$$

$$\vartheta_{2n-1}^{(-)} = \left(2n - \frac{1}{2}\right)\frac{\pi}{k},$$

with $n = 1, 2, ..., k$.

Therefore, at $\varepsilon = 0$, besides the point $(0, 0)$, $\mathscr{P}^k$ has four sets of k fixed points given in (5.53), each set corresponding to a periodic trajectory of period $k\tau_b$. Their

stability is obtained calculating the trace of the Jacobian of (5.52) at the fixed points, imposing area preservation:

$$\text{Tr} \frac{\partial(R_k, \vartheta_k)}{\partial(R_0, \vartheta_0)}\bigg|_{(\vartheta^{(\pm)}, R(0))} = 2 \pm \pi^2 (2k)^4 b C_1 \varepsilon^k \left(-\frac{1}{2C_1}\right)^k + O(\varepsilon^{k+1}). \qquad (5.54)$$

Therefore, if the sets of fixed points $(R(0), \vartheta_{2n}^{(+)})$, $(R(0), \vartheta_{2n-1}^{(+)})$ are stable, then $(R(0), \vartheta_{2n}^{(-)})$ and $(R(0), \vartheta_{2n-1}^{(-)})$ are unstable and vice versa. This corresponds to the type (b) of bifurcation presented in Tables III and V. And the proposition is proved. ∎

We now analyze the bifurcation of the harmonic V family. As already mentioned, in this case we must use the reduced Hamiltonian p_y which will then map the plane (x, p_x) on itself. Therefore, the Poincaré map in this case is obtained by imposing the symmetry $q \to -q$ $(x \to -x)$ on (5.45) which already has the symmetry $p \to -p$. In terms of variable ϑ this symmetry condition is

$$\mathscr{P} \begin{pmatrix} I_1 \\ \pi - \vartheta_1 \end{pmatrix} = \begin{pmatrix} I_0 \\ \pi - \vartheta_0 \end{pmatrix}. \qquad (5.55)$$

And we must consider two cases: k *even* and k *odd*.

If k is *even* the map is given by (5.45), which already satisfied condition (5.55).

If k is *odd*, condition (5.55) is satisfied only if $b = 0$ so that higher order terms must be considered in the reduced Hamiltonian. Up to terms of order k it is given by

$$h(I, \vartheta, t) = \varepsilon J + \sum_{j=2}^{k} C_j J^j + b J^k \cos(2k\vartheta), \qquad (5.56)$$

and the map in the lowest order approximation is given by (5.49) which automatically satisfies condition (5.55).

It is now easy to prove the

LEMMA. *Given a* vertical *periodic trajectory, if its monodromy matrix has eigenvalues* $e^{\pm 2\pi(l/k)}$, $k \geqslant 3$, $l < k$ *(l and k non-commensurate integers), then it exhibits period k-upling bifurcation. If k is* even *the bifurcation is generic (types* (a) *of Tables IV and V). If k is odd then the bifurcations are of the type given in Table VI) which is the same as type* (b) *in Tables III–V).*

Proof. The proof is immediate since if k is *even* the map is given by (5.45) and from Proposition 5.3, the bifurcation is of the generic type. Now, if k is *odd*, the map is given by (5.49) and from Proposition 5.4 the bifurcations are of the type shown in Table VI. ∎

APPENDIX

We give here a sketchy derivation of the normal form expansion [12, 13] for the Hamiltonian given in (5.7). In terms of

$$z = p + iq$$
$$\bar{z} = p - iq,$$

the reduced Hamiltonian expansion (5.7) is

$$-2ih(z, \bar{z}, t) = -\omega z\bar{z} + \sum_{m=-\infty}^{\infty} \sum_{j_1+j_2=3}^{\infty} K_{j_1 j_2 m} z^{j_1} \bar{z}^{j_2} e^{imt},$$

with $K_{j_1 j_2 m} = -\tilde{K}_{j_2 j_1 -m}$ to ensure reality of h (we have set $h_0 = 0$).

Through the time-dependent canonical transformation generated by

$$S(Z, \bar{z}) = Z\bar{z} + \sum_{\substack{m=-\infty \\ j_1+j_2=3}}^{\infty} S_{j_1 j_2 m} Z^{j_1} \bar{z}^{j_2} e^{imt},$$

the Hamiltonian in the new variables is given by

$$-2ih(Z, \bar{Z}, t) = -i\omega Z\bar{Z} + \sum_{\substack{m=-\infty \\ j_1+j_2=3}}^{\infty} \{K_{j_1 j_2 m} + i[\omega(j_1 - j_2) - m] S_{j_1 j_2 m}\}$$
$$\times Z^{j_1} \bar{Z}^{j_2} e^{imt} + \text{higher order terms (HOT)}.$$

Thus, if $\omega(j_1 - j_2) - m \neq 0$ (i.e., ω irrational), the time dependence in the lower order terms may be eliminated by choosing

$$S_{j_1 j_2 m} = \frac{iK_{j_1 j_2 m}}{m - \omega(j_1 - j_2)}.$$

The only term that could remain for irrational ω is the term $m = 0$ and $j_1 = j_2$. Therefore, for irrational ω, through successive time-dependent canonical transformation the reduced Hamiltonian can be expressed in the form

$$-2ih(z, \bar{z}, t) = -i\omega z\bar{z} + \sum_{j=2}^{N/2} K_{jj0}(z\bar{z})^j + \text{HOT}(z, \bar{z}, t),$$

to *any* desired order N. In the original variables it is

$$h(q, p, t) = \omega\left(\frac{p^2 + q^2}{2}\right) + \sum_{j=2}^{N/2} C_j\left(\frac{p^2 + q^2}{2}\right)^j + \text{HOT}(q, p, t).$$

Now, if ω is rational, $\omega = l/k$, the above expansion is not valid as it is not possible to eliminate the terms of order k that satisfy the resonance condition

$$\frac{l}{k}(j_1 - j_2) - m = 0.$$

So we have

$$-2ih(Z, \bar{Z}, t) = -i\omega Z\bar{Z} + \sum_{j=2}^{k/2} K_{jj0}(Z\bar{Z})^j$$
$$+ K_{k0l}Z^k e^{ilt} + K_{0k-l}e^{-ilt} + \text{HOT}(Z, \bar{Z}, t).$$

The resonant terms cannot be eliminated but its time dependence may be eliminated. We set $\omega = (l/k) + \varepsilon$ and make the canonical transformation

$$\xi = Ze^{i(l/k)t}, \qquad \bar{\xi} = \bar{Z}e^{-i(l/k)t},$$

which is generated by

$$\sigma = Z\bar{\xi}e^{i(l/k)t},$$

obtaining

$$-2ih(\xi, \bar{\xi}, t) = -i\varepsilon\xi\bar{\xi} - 2i\sum_{j=2}^{k/2} C_j(\xi\bar{\xi})^j + 2i\,\text{Im}(K_{k0l}\xi^k) + \text{HOT}.$$

In terms of the real coordinates J, ϑ in (5.38) the expansion is

$$h(J, \vartheta, t) = \varepsilon J + \sum_{j=2}^{k/2} C_j J^j + aJ^{k/2}\sin(k\vartheta) + bJ^{k/2}\cos(k\vartheta) + \text{HOT},$$

with $K_{k0l} = a + ib$. This expansion is valid at $\varepsilon = 0$.

REFERENCES

1. M. BARANGER AND K. T. R. DAVIES, *Ann. Phys. (N.Y.)* **177** (1987), 330

2. M. HÉNON, *Q. Appl. Math.* **27** (1969), 291; M. HÉNON AND C. HEILES, *Astron. J.* **69** (1964), 73.

3. V. A. YAKUBOVICH AND V. M. STARZHINSKII, "Linear Differential Equations with Periodic Coefficients," Keter Publishing House, Jerusalem, 1975; L. PONTRIAGUINE, "Equations Differentielles Ordinaires," Editions Mir., 1975.

4. M. BARANGER, K. T. R. DAVIES, AND J. H. MAHONEY, in preparation.

5. W. C. SAPHIR, B.S. thesis, MIT, Cambridge, MA, 1986, to be published.

6. M. A. KAGARLIS, B.S. thesis, MIT, Cambridge, MA, 1986, to be published.

7. K. R. MEYER, *Trans. Amer. Math. Soc.* **149** (1970), 95.

8. P. BONCHE, S. E. KOONIN, AND J. W. NEGELE, *Phys. Rev. C* **13** (1976), 1226; K.-K. KAN, J. J. GRIFFIN, P. C. LICHTNER, AND M. DWORZECKA, *Nucl. Phys. A* **332** (1979), 109; J. W. NEGELE, *Rev. Mod. Phys.* **54** (1982), 913; K. T. R. DAVIS, K. R. S. DEVI, S. E. KOONIN, AND M. R. STRAYER, *in* "Treatise on Heavy-Ion Science" (D. A. Bromley, Ed.), Vol. III, p. 3, Plenum, New York, 1985; PH. CHOMAS, H. FLOCARD, AND D. VAUTHERIN, *Phys. Rev. Lett.* **56** (1986), 1787; M. R. STRAYER, *in* "Proceedings of the Symposium of the ASP Topical Group on Few-Body Systems and Multiparticle Dynamics," Crystal City, Virginia, April 20–24, 1987, to be published.

9. A. K. KERMAN AND S. E. KOONIN, *Ann. Phys. (N.Y.)* **100** (1976), 332; P. KRAMER AND M. SARACENO, "Lecture Notes in Physics," Vol. 140, Springer-Verlag, New York, 1981; M. SARACENO, *Rev. Bras. Fis. Esp.* **3** (1982), 248; M. A. M. DE AGUIAR AND C. P. MALTA, *J. Chem. Phys.* **84** (1986), 6916.

10. J. GUCKENHEIMER AND P. HOLMES, *in* "Applied Mathematical Sciences," Vol. 42, Chap. 1, Springer-Verlag, New York, 1983.

11. V. I. ARNOLD, "Mathematical Methods of Classical Mechanics," Sec. 45B, Springer-Verlag, New York, 1978.

12. A. M. OZORIO DE ALMEIDA, "Hamiltonian Systems: Chaos and Quantization," in press; "Sistemas Hamiltonianos: Caos a Quantização," in press.

13. V. I. ARNOLD, "Mathematical Methods of Classical Mechanics," Appendix 7, Springer-Verlag, New York, 1978.

14. M. A. M. DE AGUIAR AND C. P. MALTA, "Isochronous and Period Doubling Bifurcations of Periodic Solutions of Non-Integrable Hamiltonians Systems with Reflexion Symmetries," in preparation.